

MODEL OF SURFACE TENSION IN THE KEYHOLE FORMATION AREA DURING LASER WELDING

ALEKSANDER SIWEK

AGH University of Science and Technology, al. A. Mickiewicza 30, 30-059 Krakow, Poland
Corresponding author: Aleksander.Siwiek@agh.edu.pl

Abstract

The nature of the laser welding process depends among others on the beam power density. Increasing the amount of energy supplied to the material, results in evolution from a shallow weld pool with flat surface, to the deep welding pool with a developed surface of the keyhole. The resulting gas/liquid surface boundary moves along with the laser beam and deforms, influenced by forces acting toward normal and tangential direction. Do not taking into account the curvature of the free surface, leads to non-physical values of the liquid velocity. In this study, for tracking and location of the interface, Volume of Fluid method (VOF) was used. It may be noted that the calculated contribution of the liquid phase, abruptly changes the value in the neighboring cells. In this paper we calculate the first and second derivatives of the liquid phase fraction function. Therefore, approximation of the normal vector and curvature of the free surface, requires the introduction of new, alternative smoothing rapid changes function. The value and direction of the force vectors were calculated, using the normal vector and curvature of the successive surface locations. The results were compared for different welding parameters.

Key words: keyhole welding, surface tension model, computational fluid dynamics (CFD), volume of fluid method (VOF)

1. INTRODUCTION

The article concerns the use of the method called volume of fluid (VOF) in the modeling of laser welding process. One of the main problems to be solved during the modeling is to track the position of the free surface separating the liquid alloy and gas. Most of the publications related to modeling of welding uses its own programs or commercial, and the VOF method for tracking the position of the boundary surface of the two phases. This method is based on the solution equation of the liquid phase fraction F . The value of this variable belongs to the range zero and one. The variable F is equal to the one in the fully melted zone, and zero in other areas. In this method negative impact on calculation result has numerical diffusion. Accuracy of solution strongly depends on the density of the mesh in the

area of the free surface. The VOF method with difficulty handles discontinuity of material properties on the phase boundary. Abrupt change of properties on the boundary are blurred. The location of the boundary determines the value of the function $F = 0.5$, and this further blurs the location. An alternative method is to formulate a Lagrange-Euler surface tracking (ALE), which updates the grid as far as free surface develops. However, this method is much more complicated to simulate in three dimensions, especially because of the remeshing in the contact zone of the two phases (Bellet & Fachinotti, 2004).

Laser welding technique used in many industrial processes involves the use of focused energy beam, to form a weld pool on the surface of the workpiece. Weld pool formation and growth depend on the characteristic of the heat source, material properties, physical phenomena in liquid metal and at interfac-

es. The choice of the laser beam mode also has an influence on the welding process (Han & Liou, 2004).

Modeling of the keyhole formation requires consideration of surface tension forces on the weld pool free surface. Inaccurate calculation of the surface curvature often lead to unrealistic flow in the vicinity of the interface and consequently abnormal shape of the boundary (Cummins et al., 2005). In the case of multiphase flow simulations, the interface position is calculated in each time step. Boundary surface consists of a partially filled elements. Mesh does not move together with the liquid. Such an approach is able to deal with highly deformed surfaces as well as the cases of joining and division of the phase boundaries (Gerlach et al., 2006). This method is of particular importance, for the modeling of keyhole welding. In particular cases during welding may occur closing of keyhole and thereby pores formation, and ejection of the molten material from the weld pool. The aim of this work is to use the VOF method to track the position of the interface, and then calculating the additional sources for the momentum equation. During welding, the gas/liquid interface influences: surface tension force (curvature), Marangoni force and recoil pressure.

2. MODEL OF SURFACE TENSION

Surface tension in two-phase flow model is treated as a continuous function of force per unit volume acting in the vicinity of the interface. The surface tension is replaced by a focused force at the interface (Williams et al., 1999). The value of this force is given by:

$$\mathbf{f}_{sv} = \mathbf{f}_{sa} \delta_s \quad (1)$$

where \mathbf{f}_{sv} surface tension force per unit volume, \mathbf{f}_{sa} surface tension force per unit of surface boundary, δ_s Dirac delta function with non-zero value only in the interface region. Surface orientation can be obtained from the definition of the Dirac function as follow (Brackbill et al., 1992):

$$\delta_s = \frac{|\nabla c|}{|c|} = |\nabla c| = |\mathbf{n}| \quad (2)$$

where c is a color function, $[c]$ step change of the color function across the interface equal to unity, \mathbf{n} vector normal to the interface. Color function is defined as follows:

$$c = \begin{cases} 1 & \text{if the element is completely filled with chosen phase} \\ 0 & \text{if the element does not contain phase} \end{cases} \quad (3)$$

The model uses volume of fluid function F as a color function. Abrupt change of the function F across the interface introduces error to the solution. Therefore volume of fluid function is smoothed in the vicinity of the interface. Averaged field \tilde{F} is obtained by convolution with a symmetrical kernel. The vector normal to the free surface is given by:

$$\mathbf{n} = \nabla \tilde{F} \quad (4)$$

The \mathbf{n} vector is calculated by the central differential scheme. Since $\nabla \tilde{F}$ is non-zero only in the interface region, also the volume force of surface tension is non-zero.

The surface force vector \mathbf{f}_{sa} is given by:

$$\mathbf{f}_{sa} = \gamma \kappa \hat{\mathbf{n}} + \nabla_s \gamma \quad (5)$$

where γ coefficient of surface tension, κ curvature of the interface, $\hat{\mathbf{n}}$ unit vector normal to the boundary surface, ∇_s gradient operator tangential to the interface.

Curvature of the interface is given by:

$$\kappa = -\nabla \cdot \hat{\mathbf{n}} = -\nabla \cdot \frac{\mathbf{n}}{|\mathbf{n}|} \quad (6)$$

Gradient operator ∇_s of the surface tension calculated by formula (5) is known as Marangoni force. The value of this gradient is related to the characteristics of the laser heat source used to the welding. Material warms up quickly near the laser beam axis. Heating rate depends on the laser mode (Han & Liou, 2004). Temperature coefficient of interfacial tension depends on the temperature and concentration of surface active elements (Sahoo et al., 1988; Rońda & Siwek, 2011). Depending on surface active element concentration and free surface temperature, coefficient $(\partial\gamma/\partial T)$ may change sign. Temperature dependence of the tangential stress $\boldsymbol{\tau}_s$ is given by:

$$\boldsymbol{\tau}_s = \nabla_s \gamma = \frac{\partial \gamma}{\partial T} \nabla_s T \quad (7)$$

It was assumed in equation (7) that at the interface, surface active element concentration is constant. The surface tension coefficient $(\partial\gamma/\partial T)$ varies along the free surface of the weld pool. Tangential component of gradient ∇_s is given by the formula (Brackbill et al., 1992):

$$\nabla_s = \nabla - \nabla_n \quad (8)$$

where ∇_n is the gradient operator in the direction normal to the interface calculated by the formula:

$$\nabla_n = \hat{\mathbf{n}} (\hat{\mathbf{n}} \cdot \nabla) \quad (9)$$



Finally, tension gradient tangent to the surface can be expressed by the formula:

$$\nabla_s \gamma = \frac{\partial \gamma}{\partial T} (\nabla T - \hat{\mathbf{n}} (\hat{\mathbf{n}} \cdot \nabla T)) \quad (10)$$

From equations (1) (5) and (10) it follows that:

$$\mathbf{f}_{sv} = \gamma \kappa \mathbf{n} + \frac{\partial \gamma}{\partial T} (\nabla T - \hat{\mathbf{n}} (\hat{\mathbf{n}} \cdot \nabla T)) |\mathbf{n}| \quad (11)$$

The above equation shows that the essence of the surface tension model, is to define the normal vector and curvature of the interface. The first force component of the equation (11) is normal to the surface and directed to the curvature center of the boundary surface. Free surface tends to reach equilibrium by changing its curvature. System seeks to achieve minimum energy by the surface shape of minimum area. Second force component of equation (11) is tangent to the surface and pointed towards an area of higher coefficient of surface tension γ (Wang, 2002). This component forces the flow at the surface of the weld pool. Knowing the dependence of the surface tension on temperature (Sahoo et al., 1988), for each solution of energy conservation equation, can be calculated force per volume of interface. Then this force is taken into account in the momentum conservation equation as a source.

3. GOVERNING EQUATIONS

The equations governing the conservation of mass, momentum and energy for incompressible Newtonian fluid are given as:

$$\nabla \cdot \mathbf{v} = 0 \quad (12)$$

$$\rho(F) \left(\frac{\partial \mathbf{v}}{\partial t} + \mathbf{v} \cdot \nabla \mathbf{v} \right) = -\nabla P + \nabla \cdot \{ \mu(F) [\nabla \mathbf{v} + (\nabla \mathbf{v})^T] \} + \rho(F) \mathbf{g} + \mathbf{f}_{sv} + \mathbf{f}_{pv} \quad (13)$$

$$\rho(F) C \left(\frac{\partial T}{\partial t} + \mathbf{v} \cdot \nabla T \right) = \nabla \cdot (k \nabla T) + \rho(F) L(F) \frac{\partial F}{\partial t} \quad (14)$$

where \mathbf{v} is the speed of the fluid, ρ is the density, P is the pressure, \mathbf{g} is the gravitational acceleration, C is the specific heat, k is the thermal conductivity, and \mathbf{f}_{pv} is the recoil due to evaporation. The volume of fluid fraction varies according to the advection equation:

$$\frac{\partial F}{\partial t} + (\mathbf{v} \cdot \nabla) F = 0 \quad (15)$$

The volume fraction of the phases in the model was initialized by a user defined function. This

function form plate inside computational domain.

Important role in the model meets the recoil. The molten metal is ejected from the laser beam area of influence, on the weld pool surface. In the impact area molten metal forms a keyhole. The shape of the keyhole depends on the interaction between volumetric force \mathbf{f}_{sv} and recoil acting on the newly created weld pool surface. Surface of the liquid reaches the temperature at which equilibrium is achieved between energy absorbed from laser beam, energy dissipated by conduction, heat of evaporation and energy contained in the ejected stream. Recoil pressure P_r is proportional to the saturation vapor pressure p_s , which is a function of the surface temperature T_s (Semak & Matsunawa, 1997; Chen & Wang, 2001; Rai et al., 2007):

$$P_r = A p_s(T_s) = A B_0 T_s^{-\frac{1}{2}} \exp\left(\frac{-U}{T_s}\right) \quad (16)$$

where A coefficient depending on pressure, B_0 empirical constant, U energy of a single atom evaporation. Thus, an additional volumetric recoil force acting on the weld pool surface is given by the equation:

$$\mathbf{f}_{pv} = \hat{\mathbf{n}} (\hat{\mathbf{n}} \cdot -\nabla P_r) \quad (17)$$

On the weld pool surface energy is balanced between the radiation source (q_{las}), keyhole surface radiation (q_{rad}), energy dissipated by convection (q_{con}) and evaporation (q_{eva}) (Zhou et al., 2006). Energy balance inside the keyhole is given by:

$$k \frac{\partial T}{\partial n} = q_{las} - q_{rad} - q_{con} - q_{eva} \quad (18)$$

Energy loss in the keyhole, describe the following equations:

$$q_{rad} = \varepsilon \sigma (T^4 - T_\infty^4) \quad (19)$$

$$q_{con} = h_c (T - T_\infty) \quad (20)$$

$$q_{eva} = W H_v \quad (21)$$

where h_c convection coefficient, ε emission factor, σ Stefan Boltzmann constant, T and T_∞ respectively the surface and the ambient temperature, H_v heat of evaporation, W rate of evaporation. For steel, the evaporation rate is calculated according to the formula (Zacharia et al., 1991):

$$\log(W) = A_v + \log(p_{atm}) - 0.5 \log(T) \quad (22)$$

where A_v constant. Steel vapor pressure p_{atm} is calculated from the following equation:



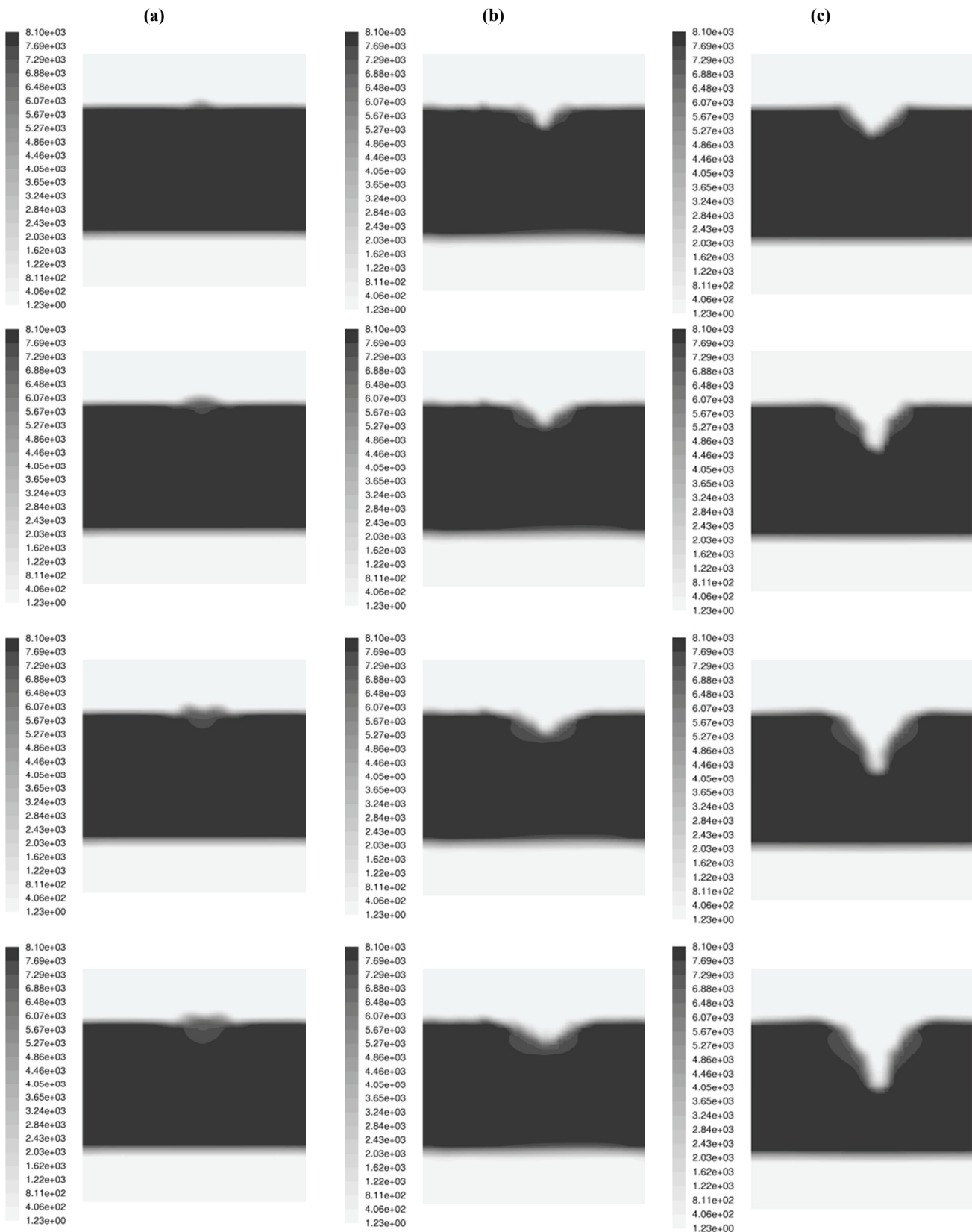


Fig. 1. Density distribution in cross sections for $P = 1 \text{ kW}$ (a), 3 kW (b) and 6 kW (c), in subsequent steps of calculations.

$$\log(p_{atm}) = 6.121 - \frac{18836}{T} \quad (23)$$

Energy flux absorbed by the surface of the sample was determined from the distribution of axially

symmetric laser beam intensity $I(x,y)$ for the TEM_{10} laser mode (Han & Liou, 2004):

$$I(x,y) = \frac{2P}{\pi a^2} \left[1 - \frac{2(x^2+y^2)}{a^2} \right]^2 \exp \left[-\frac{2(x^2+y^2)}{a^2} \right] \quad (24)$$



where P , a , x , y are respectively power, radius of the laser beam and coordinates. The laser energy is absorbed, among others by the weld pool free surface and, when keyhole is created, by the side walls of channel. The model does not take into account the effect of multiple reflection of the laser beam from the keyhole walls (Zhou et al., 2006). The energy absorbed by the wall illuminated by the laser beam is given by the equation:

$$q_{las} = \eta I(x, y) \hat{n} \cdot \hat{s} \quad (25)$$

where η absorption coefficient, \hat{s} the unit vector with the direction of the incident laser beam.

4. RESULTS AND DISCUSSION

Presented above model has been implemented in the ANSYS Fluent, a commercial software package used to model flow, turbulence and heat transfer for industrial applications. This program is based on the finite volume method for solution of transport equations. In this paper calculations were based on VOF method to solve the transport equation for dynamic viscosity, which gives stable and accurate solutions for a wide range of flows. Model was made in shape of a cube with edges equal to $4 \cdot 10^{-3}$ m. Inside the cube by means of user defined function (UDF) was formed plate with a thickness of $2 \cdot 10^{-3}$ m filled with HS 6-5-2 steel type (Rońda & Siwek, 2011). The remaining volume of the cube was filled with air. The sample was welded with a laser beam of mode TEM₁₀, $5 \cdot 10^{-4}$ m diameter and power 1, 3 and 6 kW. The laser beam was perpendicular to the upper surface of the plate and the sample moves at a constant velocity $V_y = 0.02$ m/s. The initial position of the beam coincide with the symmetry axis of the cube. Preliminary calculations helped determine the optimal finite element mesh size and the time step due to the convergence of the calculations. The sample was divided into 125000 cubic elements of the edge ~ 0017 mm. As a compromise between condition of solution convergence and the duration of the simulation, time step between two iterations was taken as 10^{-6} s. The model assumes that the sample is in normal atmospheric conditions: $p_{atm} = 101325$ Pa, $T_\infty = 300$ K. Density, specific heat, thermal conductivity and viscosity are functions of temperature. These properties

were introduced into the model as a linearly approximated discrete values in successive ranges of temperature.

Results of calculations are summarized in figure 1 as a cross-section through the computational domain, perpendicular to the x -axis. The figure contains the density distributions around the welded plate at selected moments of time. As the welding process proceed, the depth of melted zone increases (figure 2). When the laser beam power is equal to 1 kW on the surface of the molten metal forms a small cavity. Recoil is unable to exceed the surface tension force and the buoyancy force. At the liquid/gas interface equilibrium is reached between these forces. A small convexity in the last time step (figure 1a, 3a) is due to the fact that density decrease as temperature increase. For the laser beam power of 3 and 6 kW keyhole channel is formed. Increase of temperature, increases the recoil force which exceeds the force of the surface tension and then keyhole becomes deeper and narrower (figures 1b, 1c, 3b, 3c). Asymmetric geometry of the keyhole channel is due to the laser beam movement. Keyhole surface lag behind the laser beam axis, was illuminated at smaller angle.

Therefore there was supplied more of the energy (25). Energy is then transferred to the rest of weld pool by the motion of the liquid metal. Front part of the keyhole surface, illuminated by the laser beam, rapidly melts and partially evaporates. The recoil force directed normal to the liquid surface, removes

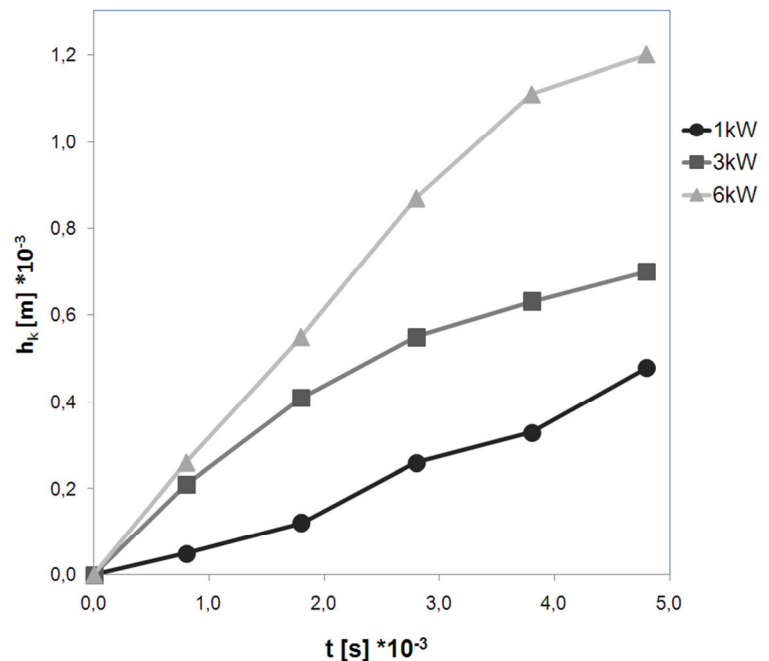


Fig. 2. Depth of the weld pool (h_k) as a function of the welding time (t) and the power of the laser beam (P).



liquid outside the laser beam impact. Shifting laser cyclically forms faults on the front surface of the keyhole. An excess of pressure inside keyhole above the ambient pressure, results the ejection of metal vapor. Keyhole remains open despite the accumulated fluid around him.

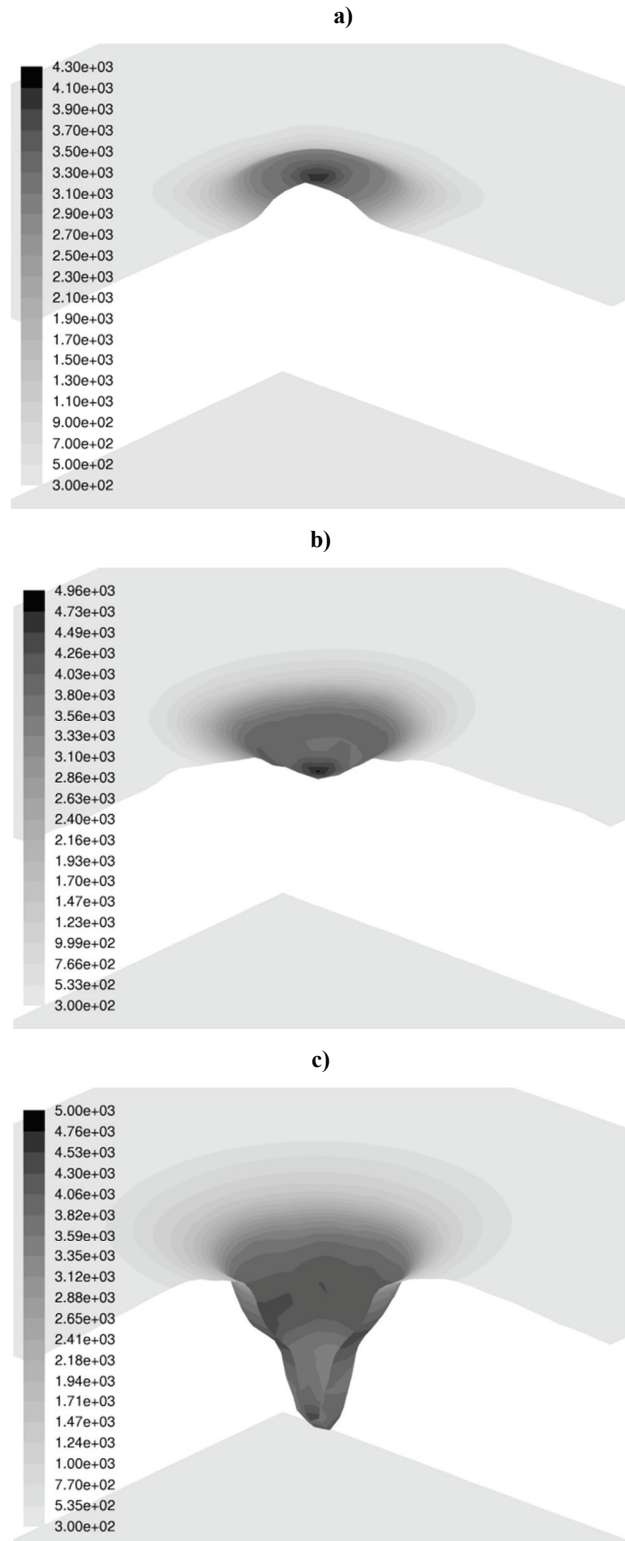


Fig. 3. Keyhole cross section for $P=1$ (a), 3 (b) and 6kW (c) at time $t = 4.8 \cdot 10^{-3}$ s. Top and bottom surface of the sample is marked with levels of gray corresponding to the temperature.

5. CONCLUSIONS

Modern keyhole models usually are developed for specific conditions and selected materials. So far, there is no precisely tested, phenomenological keyhole model, which takes into account a wide range of material types, different physical properties and different welding conditions. Still in progress work on new, more accurate models. Their accuracy largely depends on the knowledge of the temperature characteristics of the material and the physical conditions during welding.

Presented model of the surface tension during laser welding is qualitatively correct. Model runs in the conduction mode as well as in keyhole formation mode. Modeling of laser welding reduces the amount of experiments at the design stage, as well as improve process prediction and effects of the wrong parameters selection.

Acknowledgments. This publication was performed in the Academic Centre CYFRONET AGH, under the grant MNiSW/Zeus_lokalnie/AGH/084/2011.

REFERENCES

- Bellet, M., Fachinotti, V. D., 2004, ALE method for solidification modeling, *Comput. Methods Appl. Mech. Engrg.*, 193, 4355–4381.
- Brackbill, J. U., Kothe, D. B., Zemach, C., 1992 A Continuum Method for Modeling Surface Tension, *Journal of Computational Physics*, 100, 335-354.
- Chen, X., Wang, H. X., 2001, A calculation model for the evaporation recoil pressure in laser material processing, *J. Phys. D*, 34, 2637-2642.
- Cummins, S. J., Francois, M. M., Kothe, D. B., 2005, Estimating curvature from volume fractions, *Computers and Structures*, 83, 425-434.
- Gerlach, D., Tomar, G., Biswas, G., Durst, F., 2006, Comparison of volume-of-fluid methods for surface tension-dominant two-phase flows, *International Journal of Heat and Mass Transfer*, 49, 740-754.
- Han, L., Liou, F. W., 2004, Numerical investigation of the influence of laser beam mode on melt pool, *International Journal of Heat and Mass Transfer*, 4, 4385-4402.
- Rai, R., Elmer, J. W., Palmer, T. A., DebRoy, T., 2007, Heat transfer and fluid flow during keyhole mode laser welding of tantalum, Ti-6Al-4V, 304L stainless steel and vanadium, *J. Phys. D*, 40, 5753-5766.
- Sahoo, R., Debroy, T., McNallan, M. J., 1988, Surface Tension of Binary Metal Surface Active Solute Systems under Conditions Relevant to Welding Metallurgy, *Metallurgical Transactions B*, 19B, 483-491.
- Semak, V., Matsunawa, A., 1997, The role of recoil pressure in energy balance during laser materials processing, *J. Phys. D: Appl. Phys.*, 30, 2541-2552.



- Rońda, J., Siwek, A., 2011, Modelling of laser welding process in the phase of keyhole formation, *Archives of civil and mechanical engineering*, 3, 739-752.
- Wang, G., 2002, Finite Element Simulations of Free Surface Flows With Surface Tension in Complex Geometries, *Transactions of the ASME*, 124, 584-594.
- Williams, M. W., Kothe, D. B., Puckett, E. G., 1999, Accuracy and Convergence of Continuum Surface Tension Models, *Fluid Dynamics at Interface*, eds, Shyy, W., Narayanan, R., Cambridge University Press, Cambridge, 294-305.
- Zacharia, T., David, S. A., Vitek, J. M., 1991, Effect of Evaporation and Temperature-Dependent Material Properties on Weld Pool Development, *Metall. Trans. B*, 22B, 233-241.
- Zhou, J., Tsai, H. L., Lehnhoff, T. F., 2006, Investigation of transport phenomena and defect formation in pulsed laser keyhole welding of zinc-coated steels, *J. Phys. D: Appl. Phys.*, 39, 5338-5355.

MODEL NAPIĘCIA POWIERZCHNIOWEGO W OBSZARZE TWORZENIA SIĘ KANAŁU PAROWEGO W CZASIE SPAWANIA LASEROWEGO

Streszczenie

Charakter procesu spawania laserowego zależy między innymi od gęstości mocy wiązki. Zwiększenie ilości energii dostarczanej do materiału, powoduje ewolucję od płytkiego jeziora spawalniczego z płaską powierzchnią, do głębokiego jeziora z rozwiniętą powierzchnią kanału parowego. Powstała powierzchnia graniczna gaz/ciecz przemieszcza się wraz z wiązką laserową i odkształca pod wpływem sił działających w kierunku normalnej i stycznej do niej. W obszarze granicznym dwóch faz działa siła spowodowana ciśnieniem gazu, gwałtownym parowaniem, gradientem napięcia powierzchniowego i krzywizną powierzchni. Nie uwzględnienie krzywizny powierzchni rozdziału faz prowadzi do powstania błędnych wartości prędkości cieczy. W pracy do śledzenia i lokalizacji powierzchni granicznej wykorzystano metodę VOF (volume of fluid). Można zauważyć, że obliczony udział fazy ciekłej skokowo zmienia wartość w sąsiednich komórkach. W pracy obliczana jest pierwsza i druga pochodna funkcji udziału fazy ciekłej. Dlatego aproksymacja wektora normalnego i krzywizny powierzchni na podstawie udziału fazy ciekłej, wymaga wprowadzenia nowej alternatywnej funkcji wygładzającej nagłe skoki. Wartość i kierunek wektorów sił obliczano wykorzystując wektor normalny i krzywiznę w kolejnych punktach powierzchni. Porównano wyniki dla różnych parametrów spawania.

Received: November 28, 2012

Received in a revised form: December 10, 2012

Accepted: December 12, 2012

